Journal of Magnetic Resonance 241 (2014) 53–59

Contents lists available at ScienceDirect

Journal of Magnetic Resonance

journal homepage: www.elsevier.com/locate/jmr

Towards a true protein movie: A perspective on the potential impact of the ensemble-based structure determination using exact NOEs

Beat Vögeli [a,*], Julien Orts [a], Dean Strotz [a], Celestine Chi [a], Martina Minges [a], Marielle Aulikki Wälti [a], Peter Güntert [b,c], Roland Riek [a,*]

[a] Laboratory of Physical Chemistry, ETH Zurich, ETH-Hönggerberg, CH-8093 Zürich, Switzerland
[b] Institute of Biophysical Chemistry, Center for Biomolecular Magnetic Resonance, and Frankfurt Institute for Advanced Studies, J.W. Goethe-Universität, Max-von-Laue-Str. 9, 60438 Frankfurt am Main, Germany
[c] Graduate School of Science, Tokyo Metropolitan University, Hachioji, 192-0397 Tokyo, Japan

ARTICLE INFO

Article history:
Received 26 September 2013
Revised 15 November 2013

Dedicated to Prof. Dr. Christian Griesinger

Keywords:
NMR
Biological macromolecules
Proteins
Dynamics
Correlated dynamics
NOE
Nuclear Overhauser effect
eNOE
Structure calculation
Structure ensemble

ABSTRACT

Confined by the Boltzmann distribution of the energies of the states, a multitude of structural states are inherent to biomolecules. For a detailed understanding of a protein's function, its entire structural landscape at atomic resolution and insight into the interconversion between all the structural states (i.e. dynamics) are required. Whereas dedicated trickery with NMR relaxation provides aspects of local dynamics, and 3D structure determination by NMR is well established, only recently have several attempts been made to formulate a more comprehensive description of the dynamics and the structural landscape of a protein. Here, a perspective is given on the use of exact NOEs (eNOEs) for the elucidation of structural ensembles of a protein describing the covered conformational space.

1. Introduction

Proteins inherently inter-change between structural states on time scales between 10^{-12} and 10^{5} s and beyond, a process usually referred to as dynamics. As the dynamic exchanges between these states have been omnipresent during evolution, motions play an important role in the action of biomolecules. It has been suggested that concerted motions may be a pivotal factor in the enzymatic function of proteins and in protein–ligand interaction. This includes synchronization of the internal motions of a protein, which have been shown to influence the kinetics of catalysis [1,2] or to minimize entropic losses of complex formation upon ligand binding by reducing the conformational entropy of the protein [3,4]. Internal dynamics may also be involved in allosteric mechanisms [5,6]. The protein folding process is another prime example since it comprises dynamics of complex nature on large scales in both time and space. Molecular dynamics simulations, thermodynamic and kinetic studies have often been used to describe protein folding on a molecular basis [7,8].

One of the major challenges in structural biology is thus a comprehensive description of the 3D structures and the exchange dynamics between structural states at atomic resolution with the ultimate goal of an experimental data-based movie of a biomolecule. While structure determination of biomolecules at atomic resolution by NMR or X-ray crystallography is well established, the description of structural landscapes of proteins as well as the dynamic interchange between the various conformations are still largely incomplete. Routine analysis of fast and slow local dynamics is done by means of relaxation measurements and is mostly restricted to backbone ^{15}N–^{1}H moieties but increasingly includes methyl groups [9,10]. However, there is exciting progress in NMR-based methods towards a more holistic description of structural landscapes of proteins and the transitions between the various states. These include measurements of residual dipolar couplings (RDCs) [11], relaxation dispersion (CPMG) [12], cross-correlated relaxation (CCR) [13,14], paramagnetic relaxation

* Corresponding authors. Fax: +41 1 633 10 73.
E-mail addresses: beat.voegeli@phys.chem.ethz.ch (B. Vögeli), roland.riek@phys.chem.ethz.ch (R. Riek).

1090-7807/$ - see front matter © 2013 Elsevier Inc. All rights reserved.
http://dx.doi.org/10.1016/j.jmr.2013.11.016

enhancement (PRE) [15], and exact nuclear Overhauser enhancement (eNOE) data [16,17], in combination with molecular dynamics simulation, structure prediction software, or ensemble-based structure calculations [18–23].

In the following, we present a perspective on the recently introduced protocol of ensemble-based structure determination with ensemble-averaged distance restraints obtained from exact NOE rates [17,22–26] and highlight its potential impact in the comprehensive elucidation of the action of biomolecules at atomic resolution.

2. The eNOE in the 3D structure determination

2.1. From NOESY spectra to distance restraints

The NOE cross-relaxation rate between two spins ½ K and L is given by [27,28]

$$\sigma_{KL} = \left(\frac{\mu_0}{4\pi}\right)^2 \frac{\gamma^4 h^2}{40\pi^2} \frac{1}{\left(r_{KL}^{\text{rigid}}\right)^6} [J(0) - 6J(2\omega)] \tag{1}$$

where γ is the gyromagnetic ratio of nucleus K, ω is the spectral frequency of the nuclei, μ_0 is the permeability in vacuum, and h denotes Planck's constant. r_{KL}^{rigid} is the internuclear distance in a hypothetically rigid structure. A simple expression for the spectral density J obtained under the assumption of isotropic molecular tumbling [27] is

$$J(\omega) = S_{KL}^{\text{fast2}} \frac{\tau_c}{1 + (\tau_c\omega)^2} + \left(\left(r_{KL}^{\text{rigid}}\right)^6 \left\langle \frac{1}{r_{KL}^6} \right\rangle - S_{KL}^{\text{fast2}}\right) \frac{\tau_{\text{tot}}}{1 + (\tau_{\text{tot}}\omega)^2} \tag{2}$$

with

$$\frac{1}{\tau_{\text{tot}}} = \frac{1}{\tau_c} + \frac{1}{\tau_{\text{int}}} \tag{3}$$

where τ_c is the rotational correlation time of the molecule and τ_{int} is the correlation time for internal motion. The angle brackets denote a Boltzmann ensemble average and S_{KL}^{fast2} is an order parameter for fast internal motion [29],

$$S_{KL}^{\text{fast2}} \equiv \left(r_{KL}^{\text{rigid}}\right)^6 \frac{4\pi}{5} \sum_{q=-2}^{2} \left\langle \frac{Y_{2q}\left(\theta_{KL}^{\text{mol}}, \phi_{KL}^{\text{mol}}\right)}{(r_{KL})^3} \right\rangle^2 \tag{4}$$

(Note that the influence of anisotropic tumbling can be neglected in most cases as discussed in Ref. [24]).

It is evident from Eqs. (1)–(4) that the NOE is a time- and ensemble-averaged observable containing both structural and dynamical information. However, the most common way to extract distances from the measured NOE cross-relaxation rate is to assume the presence of a rigid molecule $\left(\text{i.e. } S_{KL}^{\text{fast2}} = 1 \text{ and } \left\langle \frac{1}{r_{KL}^6} \right\rangle = \frac{1}{\left(r_{KL}^{\text{rigid}}\right)^6}\right)$. This simplification of the theory is usually accompanied by the assumption that the NOE rate is proportional to the cross peak intensity in NOESY spectra. However, the apparent cross peak intensities are also influenced by peak overlap, relaxation during the mixing period and most importantly by spin diffusion, which is the indirect magnetization transfer between the two spins of interest via other nearby spins. Because of these effects, NOE cross peaks from NOESY spectra are usually translated semi-quantitatively into upper limit distances, following the proportionality of the NOE cross-relaxation rate with the inverse 6th power of the distance between two (isolated) interacting spins (Eq. (1)) [28,30]. This practice originates from the 1980s when it proved difficult to determine NOE rates and to convert them into exact distances [28,30].

Today's procedures to measure and interpret NOEs are barely more sophisticated than those outlined above, despite of all the progress in NMR including (i) the availability of high magnetic fields and heteronuclear spectroscopy (i.e. ^{15}N and ^{13}C-resolved [^{1}H, ^{1}H]-NOESY) which reduce peak overlap significantly, (ii) the considerable increase in sensitivity due to cryoprobe technology, which enables the use of shorter NOE mixing times in order to reduce the spin diffusion substantially (note, the desired contribution to the cross peak grows linearly with the mixing time, while the contribution from spin diffusion increases with the square of the mixing time), and (iii) increased computer power enabling analytical advances such as the full relaxation matrix formalism applied to the Solomon equation in order to correct NOE restraints for spin diffusion [25,31,32]. In light of these advances, paralleled with the notion that the translation from NOE rates to distances is very robust because the $1/r^6$ dependency between NOE and distance reduces the relative distance error sixfold compared to the relative inaccuracies of the NOE measurements [24], we have recently revisited the NOE measurements and analysis on both deuterated [17] and protonated protein samples [24]. The collection of exact $^1H^N$–$^1H^N$ NOE rates (eNOEs) was achieved by using a high field NMR spectrometer (i.e. 700 MHz) with a cryoprobe, optimized 3D-resolved [^{1}H, ^{1}H]-NOESY experiments, short NOESY mixing times, and an optimized protocol for extracting NOE rates from a series of NOESY spectra accompanied by correction for spin diffusion as described in Fig. 1. The NOE rates were converted into distances by making use of the relative insensitivity of the NOE to fast motion (i.e. $S_{KL}^{\text{fast2}} = 1$ in Eqs. (1)–(4)), which was shown to be valid for H–H spin pairs if the local H–X order parameters for fast motion are larger than 0.5 [33]. This is most often the case in folded proteins (see also below). In these studies, an experimental random error of 0.07 Å demonstrated that distances up to 5 Å can be derived from eNOEs with high accuracy. This error is considerably smaller than the 0.24 Å pairwise root mean square (rms) deviations from distances extracted from corresponding high-resolution NMR or X-ray structures. These initial studies indicated that exact NOEs (eNOEs) can be collected and converted into precise distance restraints.

2.2. From the eNOE-derived distance restraints to the 3D structural ensemble

A data set of more than 800 eNOEs was established for the model protein GB3 [22,23]. The eNOE-derived distance restraints in combination with a small set of RDCs and torsion angle restraints derived from scalar couplings and $^{13}C^{\alpha}$ chemical shifts were then used for a structure calculation following standard protocols. A bundle of nine conformers is shown in Fig. 2, middle. The exact nature of the eNOE results in an extremely tight structure bundle (with a root-mean-square deviation for the backbone atoms of 0.11 Å), in particular when compared to a conventional structure calculation using semi-quantitative NOEs (compare Fig. 2 left with middle) and coincides closely with the RDC-optimized X-ray structure [35,36]. However, there are many distance restraint violations indicating that the structure does not agree with the experimental data. The large number of violations of experimental restraints is attributed to the motion-averaged nature of the measured NOE (Eqs. (1)–(4)) since the structure calculation protocol is based on a single static structure.

According to the ergodic hypothesis, the impact of protein motion on the NOE measurement can be described by an ensemble of structural states. To include the dynamic dependence of the eNOEs in the structure calculation (Eqs. (1)–(4)), an ensemble-based protocol was established (within the software package CYANA). The protocol requests that the experimental restraints are fulfilled by a set of structural states rather than by a single structure. In

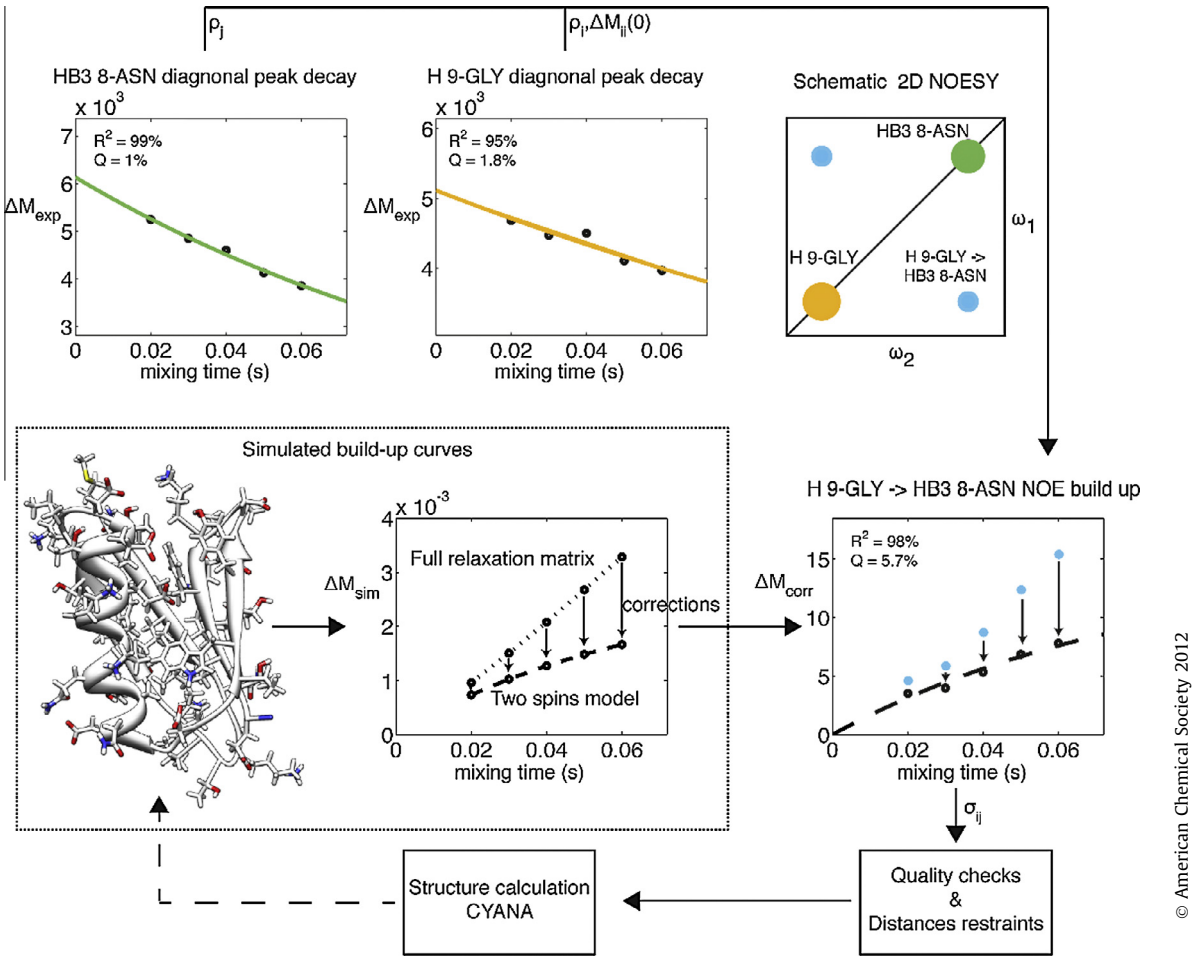

Fig. 1. Flow chart representing the method for the determination of eNOEs and the structure calculation with eNOEs. As an example, the eNOE originating from the amide H of Gly9 (spin *i*, orange) and enhancing $H^{\beta 3}$ of Asn8 (spin *j*, green) of GB3 is shown. (1) The diagonal peak intensities derived from the NOESY spectra are fitted to mono-exponential decay functions to extract the auto-relaxation rate constants, ρ_i, ρ_j, and the initial magnetization on spin *i*, $\Delta M_{ii}(0)$. (2) A build-up curve taking into account all magnetization pathways is simulated with the full relaxation matrix approach. This simulation requires a 3D structure as input, which may be based on a conventionally determined NMR structure or an X-ray structure. (3) Corrections for the intensities at each mixing time are applied to the experimental NOE build-up. (4) The NOE build-up is fitted, the quality of the fit is evaluated and upper and lower bound distance restraints are created. (5) A structure calculation is performed with the new distance restraints using established software packages such as CYANA [26,34]. This structure may be used as an input for (2) in a new cycle as indicated by the broken arrow. Adapted with permission from Orts, Vögeli, Riek, J. Chem. Theory Comput. 8 (2012) 3483–3492 [25].

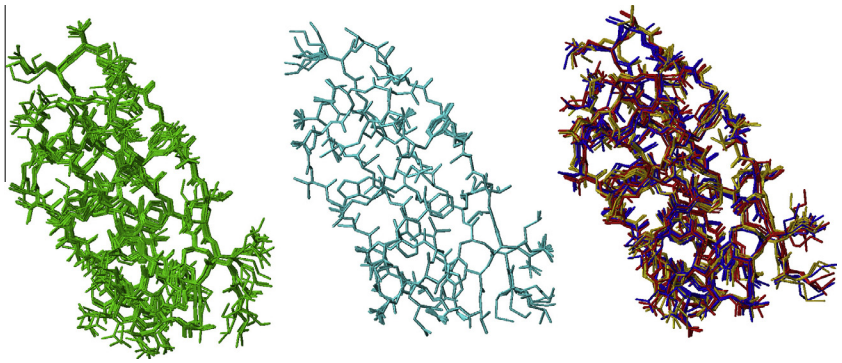

Fig. 2. Heavy-atom structural representations of GB3 following either the conventional protocol with NOEs as experimental input, the conventional protocol with eNOEs or the ensemble-based protocol with eNOEs. Left: Bundle calculated with a conventional protocol based on standard NOE measurements. Nine conformers are shown. Middle: Single-state bundle calculated with eNOEs. Nine conformers are shown. Right: 3 three-state ensembles obtained from eNOEs. The three most similar structures from each three-state conformer are grouped in gold, red and blue. Reprinted by permission from: Vögeli, Kazemi, Güntert, Riek, Nat. Struct. Mol. Biol. 19 (2012) 1053–1057 [22].

contrast to the standard structure determination protocol, it therefore takes into account that the NOE is a time and ensemble-averaged parameter. To avoid divergence among the structural states that is not implied by the experimental restraints, we impose "bundling restraints", i.e. weak harmonic restraints that minimize the distances between corresponding atoms in different states [37]. Using this protocol, it is found that the ensemble consisting of three three-state structures shown in Fig. 2 describes the

experimental data well. This structural ensemble is a compact experiment-based representation of GB3 covering its conformational space in solution. Because of the bundling restraints used for the calculation, the ensemble covers the minimal conformational space required to fulfill the experimental data.

A detailed inspection of the structural ensemble shows that the three structural states are distinct from each other (Fig. 2, right) with pronounced differences for the β-sheet and attached loops (Fig. 3). The timescale of exchange is most likely on the sub-ms time scale, because slower motions would result in line broadening or resonance doubling that is not observed in the spectra, and because the three-state ensemble is in fair agreement with the RDC-derived order parameters that are sensitive to motion faster than milliseconds [36]. These interpretations indicate that the entire β-sheet and some of the loops undergo a conformational exchange between the three states in a concerted fashion. The central β-sheet strands (β1 and β4) move parallel to the entire β-sheet architecture (i.e. vertically to the polypeptide backbone), while the loops β1/β2, and β3/β4 as well as accompanied segments within the β-strands counteract this motion in an anti-correlated manner. A principal component analysis of the ensemble visualizes these findings further [22] and the described ensemble is in good agreement with previously obtained multiple-state ensembles [18,38]. The ensemble reveals further insights into structure and dynamics such as side chain rotamer states, conformational exchange dynamics of the side chains, and correlation between backbone and side chain configurations (for more details see Ref. [23]).

3. Challenges and limitations

There are a few challenges and limitations on measuring highly precise and accurate NOEs (eNOEs) and their simple conversion into precise averaged distances. The most important ones are discussed in the following, while others are listed in Refs. [23,40].

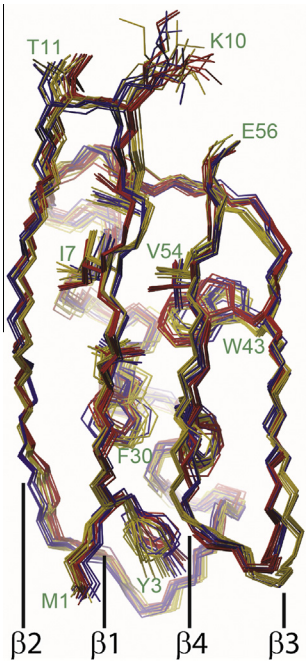

Fig. 3. The 3D ensemble structure of GB3. Representation of three states of GB3 obtained from the ensemble-based protocol using eNOEs. The three most similar structures from each three-state conformer are grouped in gold, red and blue. For each ensemble 9 conformers were selected. The backbone, the side chains of the hydrophobic core and the two solvent-exposed residues K10 and T11 are also shown. The termini and the side chains are labeled with the residue number. Figure is taken from Vögeli, Orts, Strotz, Güntert, Riek, Chimia 66 (2012) 787–790 [39].

3.1. The complex time dependency of the NOE

In the present translation from eNOE rates to distances it is assumed that fast motion (i.e. faster than the rotational correlation time of the protein studied) does not perturb the NOE (i.e. $S^{fast2}_{KL} = 1$ in Eqs. (1)–(4)). The rational of this assumption is based on the finding that for H–H NOEs between two H–X moieties (X being a heavy atom) with order parameters larger than 0.5 the NOE is indeed not influenced significantly by fast motions because the fast motion-induced angular and distance effects on the NOE rate cancel each other almost entirely [33]. Similar conclusions have been drawn from molecular dynamics studies, but they also reveal that a few percent of the NOEs may violate the assumption considerably yielding distances with an error of more than 10% [27,41]. In the first study [27], a detailed analysis showed that these critical NOEs are from side chain atoms of a phenylalanine. In the second study [41], half of the critical NOEs involve side-chain arginine and lysine protons and not surprisingly, the most extreme averaging involves dihedral transitions. Conclusively, NOEs involving atoms located at the far end of very long, highly flexible side chains must be used with caution. Whether a combination of exact NOESY and ROESY measurements [27] or the measurements of local order parameters of each $^{1}H–^{15}N$ and $^{1}H–^{13}C$ moiety by ^{15}N- and ^{13}C-relaxation measurements, respectively, and $^{13}C–^{13}C$ NOESY [42] may resolve these potential source of error remains to be demonstrated. It must be noted however, that the strongest driving force in the ensemble structure calculation is the cumulative impact of a dense network of eNOEs which should reveal or cancel the effect of such potentially incorrect distance measurements.

3.2. Limitations on the system size studied

Our investigations on eNOEs have been conducted on the two small model proteins GB3 and ubiquitin (i.e. 6.5 and 8.5 kDa, respectively). Larger systems pose two potential challenges. First, large systems have long overall correlation times, which cause stronger transverse relaxation effects. As a consequence, magnetization is lost along the pathways during the pulse sequence. Longitudinal relaxation is reduced and thus the inter-scan delays must be increased. However, as the NOE transfer relies on longitudinal magnetization and is proportionally more efficient with increasing overall tumbling times, NOESY belongs to the group of experiments that can be used on very large systems.

The second major limitation is caused by increased peak overlap for large systems. The problem is particularly pressing with respect to the diagonal peaks, which must be analyzed in order to obtain the magnetization at the onset of NOESY mixing, ΔM, and the auto-relaxation rate ρ depicted in Fig. 1. Recording NOESY spectra with additional dimensions, such as 4D HMQC-NOESY-HMQC types [43] would partially resolve the diagonal peak overlap by separating the two proton shifts by two heavy atom resonances [43]. Whether sparse sampling techniques [44,45] in combination with special spectral transformation schemes (such as compressed sensing reconstruction [45] or the SCRUB algorithm [46]) may be applicable remains to be demonstrated because the cross peak and diagonal peak intensities must be preserved for the extraction of eNOE rates.

3.3. Cross validation of the eNOEs and the problem of incorrect assignments

NMR structure determination is a multi-probe method that requires hundreds to thousands of experimental restraints for a reliable structure determination. Among the large number of restraints, there will, in general, be some incorrect ones. Wrong

restraints may originate, for example, from wrong assignments or/and wrong integration caused by peak overlap. In a standard structure determination, these artifact restraints are usually exposed by distance restraint violations in the resulting 3D structure (such as a large contribution to the target function in the software package CYANA). In an ensemble-based structure calculation, on the other hand, they may be hidden and even lead to the appearance of an additional structural state. A cross validation procedure for the ensemble-based structure calculation using eNOEs is therefore mandatory. In our recent work, this test consisted of the arbitrary deletion of 10% of all the eNOE-derived distance restraints and a subsequent consistency check by evaluating their violations with a structural ensemble obtained from the remaining 90% restraints (i.e. contribution to the target function) [47]. Although this approach is sound, more profound studies should be designed for the identification of wrong eNOEs and their potential influence, such as the inferential structure determination by Bayesian inference to derive a probability distribution [48,49].

3.4. Combining various NMR experimental restraints for ensemble-based structure calculation

At present, exciting progress is witnessed in NMR-based methods employing RDC, PRE, CCR and eNOE restraints with the aim of a comprehensive description of a protein's structure and dynamics at atomic resolution. While independent applications of these methods currently prevail, each method has its merrits. They cover different time scales, are applied to different atomic moieties (such as backbone $^{1}H–^{15}N$ or side chain $^{1}H–^{13}C$ moieties), are sensitive to either rotational or translational motion and configurations (or both), and are either of local (for example NOE) or of global nature (for example RDC). Some of them are sensitive to rather small populations (for example chemical shifts and PRE), while others are sensitive to concerted motion (for example CCR). These different sets of probes must be considered in light of the many degrees of freedom of a dynamic multi-atomic macromolecule on time scales covering many order of magnitudes. This complexity renders the back-transformation from the measured data to its (dynamic) origin ambiguous. It is therefore evident that these methods must be combined for a comprehensive description of a protein's structure and motion at atomic resolution. However, in virtually all ensemble refinement protocols NMR observables are averaged in a uniform manner irrespective of the time windows they are sensitive to. To make things even worse, the NOE rate averages differently over short and long time scales, and the practical choice of averaging (r^{-6} versus r^{-3}) seems rather heuristic in most publications (see also above). However, an adquate combined implementation should be feasible because it is not hindered by fundamental theoretical considerations. For example, assuming experimental knowledge at all relevant time scales were available, one may restrain molecular dynamics simulations with all the experimental data in correctly time-averaged fashion yielding an ensemble of protein movies similar to the ensemble description of NMR structures, but time resolved.

4. Perspectives

Precise and accurate NOEs (eNOEs) can readily be measured and converted into exact averaged distances. eNOE-based structural ensembles open an avenue to the determination of structural landscapes of proteins. Such landscapes are indispensible for the establishment of comprehensive structure–dynamics–activity relationships. Aspects that may be studied with the eNOE approach are manifold: protein folding, enzymatic activities, allosteric regulation, protein–ligand interaction and characterization of intrinsically disordered proteins. In the following, current projects in our laboratory that illustrate these applications are outlined.

The folding of a protein from its random coil-like state (or nascent chain) into its well folded compact 3D structure is one of the most complex biological processes and not yet fully understood [8,50]. The three-stranded β-sheet mini fold of the WW domain, composed of 34 residues, is often used in protein folding studies. A wealth of mutagenesis, kinetic, NMR and thermodynamic measurements along with molecular dynamics simulations [51–54] illustrate the complexity of its folding. Some data indicate a turn-initiated folding and β-sheet formation in a zipper-like fashion. Other experiments and molecular dynamic simulations (MD) have shown that the relative weight of rate limiting features shifts from loop 1 to loop 2 with changes in experimental conditions such as temperature [55,56]. Other MD simulations are in conflict with experimental results and claim that the hydrophobic cluster might be labile during unfolding [57,58] and that some native contacts could shape folding pathways [56]. Again other simulations show a rapid hydrophobic collapse or predict the existence of multiple pathways [54,59]. It is evident that eNOE measurements of the WW domain at temperatures close to the melting temperature, at which the protein folds and unfolds rapidly (i.e. faster than ms), have the potential to yield ensemble-averaged data with the principle possibility to determine a structural ensemble of the WW domain that resembles the folding pathway (including the folded state). A combination of eNOE measurements with other NMR-based probes sensitive to protein folding such as relaxation dispersion experiments [60] and RDCs [11,61] is thereby desirable.

In a second application, eNOEs may also be used to characterize intrinsically disordered proteins (IDPs) [50,62,63]. Conventional NOEs have been used to identify propensities of residual secondary structural features [64–66]. However, as few or no long-range NOEs are observed, structural restraints for IDPs are sparse. Due to their high accuracy in distance determination, eNOEs have the potential to provide unprecedented insights. To test the applicability of eNOEs, we have recorded NOESY series on amyloid beta Aβ (1-42) in aqueous solution [67–70]. Our findings in Aβ peptide correlate with the β sheet- and random coil-like regions found in Aβ amyloids, fibrillized under the same solution conditions (unpublished).

Third, the notion that enzyme activity is regulated by conformational sampling offers another interesting application for the eNOE methodology. The enzyme prolyl cis–trans isomerase cyclophilin A has been shown by NMR relaxation experiments, mutagenesis, and kinetic measurements to undergo population shifts in times scales correlated with its activity via a complex dynamic network [71–74]. The sampling frequencies corresponding to the turnover rates of the catalytic reaction are also observed in the apo state as confirmed with side directed mutants [75–77]. Furthermore, mutagenesis studies indicated that part of these motions is of concerted nature. In order to unravel the action of an enzyme, we attempt to obtain insight at atomic resolution from the eNOE-based determination of an ensemble of structural states in presence and absence of the substrate. In principle, this should be possible because the measured eNOEs of the enzyme in presence of substrate are averaged over the substrate-free state, substrate-bound state before catalysis, transition state (although this state may be too short lived for a considerable contribution to the eNOE) and substrate-bound state after catalysis, and possibly other intermediate states. For this endevaour, again, the eNOE measurements should be complemented with other NMR-based probes including relaxation measurements.

Another subject for which the eNOE-based ensemble structure determination may be able to give detailed insight is the possible concerted dynamic nature of allosteric regulations. PDZ domains (post-synaptic density-95/disks large/zonula occludens-1) are highly abundant modules that mediate protein–protein interactions

in eukaryotes such as organizing signaling pathways [78,79]. They have been proposed to exhibit long-range evolutionary, energetic, structural and dynamical couplings that link distant molecular docking sites [80–85]. Such global interaction networks can be mapped with sequence-based statistical methods, double mutant cycle analysis and NMR structural and relaxation studies [80–85]. Changes in backbone amide and side-chain methyl relaxation rates upon peptide binding and mutagenesis were linked to allosteric behavior [82,83,86,87]. In addition, comparison of methyl relaxation data of different PDZ domains gave evidence for conserved side-chain dynamics [88]. NMR data including conventional NOEs and the backbone amide and side-chain methyl relaxation rates has also been used to restrain molecular dynamics (MD) simulations [89]. However, the evolutionary network does not coincide with any of the MD-detected networks but corresponds more closely to the dynamical network proposed [80]. Under a more general view, the determination of structural ensembles using eNOEs, RDCs and other structural restraints may contribute significantly to the understanding of the origin of allosteric regulation as illustrated here with the case of the PDZ domains.

Finally, it is emphasized that the use of inter-molecular eNOEs between a substrate and the protein may not only give insight into the 3D structure, but also into the dynamics of the interaction site due to the time-averaged and ensemble-averaged nature of the eNOE. The analysis of inter-molecular eNOEs between a substrate and its protein partner may thus reveal intermolecular motions, which can possibly be translated into local entropic contributions to binding energies. Furthermore, they may indicate the presence of domain or secondary structure motions as exemplified by our recent eNOE analysis of membrane protein-detergent NOEs [90]. Their analysis suggested the presence of helical motions in two helical membrane proteins including a deletion variant of the membrane-attached hemaglutinin HAfp [90,91]. The nature of the dynamics might be either helix rotation or partial unfolding of the tertiary structure that increases the contact surface of a transmembrane or a membrane-attached helix with its membrane mimetic.

5. Conclusion

The experiment-based characterization of dynamics of a biomolecule is usually of descriptive manner and as such limited. However, combining the recently established NMR-based methods using RDCs, PREs, CCRs and eNOEs for the study of protein structure and dynamcis opens the avenue towards a coordinate-based and time-resolved quantitative description of a protein's action. The information content on dynamics would be far superior to that of local relaxation rate measurements or chemical shift changes as it would reflect or ideally yield an experiment-based protein movie of quantitative nature. Such movies would represent key scenes from the life of a protein with a precision determined by the measured constraints. It is our opinion that such experimental data-based protein movies of biological relevant systems may contribute significantly to our understanding of biology and in particular of the multi-dimensional complex protein structure-dynamics-activity relationship of biomolecules.

Acknowledgments

We thank the Swiss National Foundation for financial support. B.V. was supported by the Swiss National Science Foundation with Grant 140214 and the by ETH Research Grant ETH-04 13-1, and C.C. by a Vetenskap Lådet (VR) post doc fellowship, respectively. P.G. gratefully acknowledges financial support by the Lichtenberg program of the Volkswagen Foundation. Some of the text passages used may originate from other recent publications from the authors [17,22–25,33,39,40].

References

[1] T.C. Bruice, S.J. Benkovic, Chemical basis for enzyme catalysis, Biochemistry 39 (2000) 6267–6274.
[2] M.J. Osborne, J. Schnell, S.J. Benkovic, H.J. Dyson, P.E. Wright, Backbone dynamics in dihydrofolate reductase complexes: role of loop flexibility in the catalytic mechanism, Biochemistry 40 (2001) 9846–9859.
[3] K.K. Frederick, M.S. Marlow, K.G. Valentine, A.J. Wand, Conformational entropy in molecular recognition by proteins, Nature 448 (2007) 325–329.
[4] S.-R. Tzeng, C.G. Kalodimos, Protein activity regulation by conformational entropy, Nature 488 (2012) 236–240.
[5] R.K. Jain, R. Ranganathan, Local complexity of amino acid interactions in a protein core, Proc. Natl. Acad. Sci. USA 101 (2003) 111–116.
[6] P. Weinkam, J. Pons, A. Sali, Structure-based model of allostery predicts coupling between distant sites, Proc. Natl. Acad. Sci. USA 109 (2012) 4875–4880.
[7] D.E. Shaw, P. Maragakis, K. Lindorff-Larsen, S. Piana, R.O. Dror, M.P. Eastwood, J.A. Bank, J.M. Jumper, J.K. Salmon, Y. Shan, W. Wriggers, Atomic-level characterization of the structural dynamics of proteins, Science 133 (2011) 341–346.
[8] C. Eichmann, S. Preissler, R. Riek, E. Deuerling, Cotranslational structure acquisition os nascent polypeptides monitored by NMR spectroscopy, Proc. Natl. Acad. Sci. USA 107 (2010) 9111–9116.
[9] L.E. Kay, D.A. Torchia, A. Bax, Backbone dynamics of proteins as studied by nitrogen-15 inverse detected heteronuclear NMR spectroscopy: application to staphylococcal nuclease, Biochemistry 28 (1989) 8972–8979.
[10] L.E. Kay, NMR studies of protein structure and dynamics, J. Magn. Reson. 173 (2005) 193–207.
[11] L. Salmon, G. Bouvignies, P. Markwick, M. Blackledge, Nuclear magnetic resonance provides a quantitative description of protein conformational flexibility on physiologically important time scales, Biochemistry 50 (2011) 2735–2747.
[12] A. Mittermaier, L.E. Key, New tools provide new insights in NMR studies of protein dynamics, Science 312 (2006) 224–228.
[13] D. Frueh, Internal motions in proteins and interference effects in nuclear magnetic resonance, Prog. Nucl. Magn. Reson. Spectrosc. 41 (2002) 305–324.
[14] B. Vögeli, L. Yao, Correlated dynamics between protein HN and HC bonds observed by NMR cross relaxation, J. Am. Chem. Soc. 131 (2009) 3668–3678.
[15] J. Iwahara, G.M. Clore, Structure-independent analysis of the breadth of the positional distribution of disordered groups in macromolecules from order parameters for long variable-length vectors using NMR paramagnetic relaxation enhancement, J. Am. Chem. Soc. 132 (2010) 13346–13356.
[16] T.M.G. Koning, R. Boelens, R. Kaptein, Calculation of the nuclear Overhauser effect and the determination of proton-proton distances in the presence of internal motion, J. Magn. Reson. 90 (1990) 111–123.
[17] B. Vögeli, T.F. Segawa, D. Leitz, A. Sobol, A. Choutko, D. Trzesniak, W. van Gunsteren, R. Riek, Exact distances and internal dynamics of perdeuterated ubiquitin from NOE buildups, J. Am. Chem. Soc. 131 (2009) 17215–17225.
[18] G.M. Clore, C.D. Schwieters, Amplitudes of protein backbone dynamics and correlated motions in a small alpha/beta protein: correspondence of dipolar coupling and heteronuclear relaxation measurements, Biochemistry 43 (2004) 10678–10691.
[19] K. Lindorff-Larsen, R.B. Best, M.A. DePristo, C.M. Dobson, M. Vendruscolo, Simultaneous determination of protein structure and dynamics, Nature 433 (2005) 128–132.
[20] O.F. Lange, N.A. Lakomek, C. Farès, G.F. Schröder, K.F.A. Walter, S. Becker, J. Meiler, H. Grubmüller, C. Griesinger, B.L. de Groot, Self-consistent residual dipolar coupling based model-free analysis for the robust determination of nanosecond to microsecond protein dynamics, Science 320 (2008) 1471–1475.
[21] R.B. Fenwick, S. Esteban-Martin, B. Richter, D. Lee, K.F.A. Walter, D. Milanovic, S. Becker, N.A. Lakomek, C. Griesinger, X. Salvatella, Weak long-range correlated motions in a surface patch of ubiquitin involved in molecular recognition, J. Am. Chem. Soc. 133 (2011) 10336–10339.
[22] B. Vögeli, S. Kazemi, P. Güntert, R. Riek, Spatial elucidation of motion in proteins by ensemble based structure calculation using exact NOEs, Nat. Struct. Mol. Biol. 19 (2012) 1053–1057.
[23] B. Vögeli, P. Güntert, R. Riek, Multiple-state ensemble structure determination from eNOE spectroscopy, Mol. Phys. 111 (2012) 1–18.
[24] B. Vögeli, M. Friedmann, D. Leitz, A. Sobol, R. Riek, Quantitative determination of NOE rates in perdeuterated and protonated proteins: practical and theoretical aspects, J. Magn. Reson. 204 (2010) 290–302.
[25] J. Orts, B. Vögeli, R. Riek, Relaxation matrix analysis of spin diffusion for the NMR structure calculation with eNOEs, J. Chem. Theory Comput. 8 (2012) 3483–3492.
[26] J. Orts, B. Vögeli, R. Riek, P. Güntert, Stereospecific assignments in proteins using exact NOEs, J. Biomol. NMR 57 (2013) 211–218.
[27] R. Brüschweiler, B. Roux, M. Blackledge, C. Griesinger, M. Karplus, R.R. Ernst, Influence of rapid intramolecular motion on NMR cross-relaxation rates. A molecular dynamics study of antamanide in solution, J. Am. Chem. Soc. 114 (1992) 2289–2302.
[28] D. Neuhaus, M.P. Williamson, The Nuclear Overhauser Effect in Structural and Conformational Analysis, Wiley, New York, 2000.
[29] G. Lipari, A. Szabo, Model-free approach to the interpretation of nuclear magnetic resonance relaxation in macromolecules. 1. Theory and range of validity, J. Am. Chem. Soc. 104 (1982) 4546–4559.
[30] K. Wüthrich, NMR of Proteins and Nucleic Acids, Wiley, New York, 1986.

[31] I. Solomon, Relaxation processes in a system of two spins, Phys. Rev. 99 (1955) 559–565.
[32] R. Boelens, T.M.G. Koning, G.A. Vandermarel, J.H. Vanboom, R. Kaptein, Iterative procedure for structure determination from proton–proton NOEs using a full relaxtion matrix approach. Application to a DNA octamer, J. Magn. Reson. 82 (1989) 290–308.
[33] D. Leitz, B. Vögeli, J. Greenwald, R. Riek, Temperature dependence of 1HN-1HN distances in ubiquitin as studied by exact measurements of NOEs, J. Phys. Chem. B. 115 (2011) 7648–7660.
[34] P. Güntert, Automated structure determination from NMR spectra, Eur. Biophys. J. 38 (2009) 129–143.
[35] T.S. Ulmer, B.E. Ramirez, F. Delaglio, A. Bax, Evaluation of backbone proton positions and dynamics in a small protein by liquid crystal NMR spectroscopy, J. Am. Chem. Soc. 125 (2003) 9191–9197.
[36] L. Yao, B. Vögeli, D.A. Torchia, A. Bax, Simultaneous NMR study of protein structure and dynamics using conservative mutagenesis, J. Phys. Chem. B 112 (2008) 6045–6056.
[37] G.M. Clore, C.D. Schwieters, How much backbone motion in ubiquitin is required to account for dipolar coupling data measured in multiple alignment media as assessed by independent cross-validation?, J Am. Chem. Soc. 126 (2004) 2923–2938.
[38] G.M. Clore, C.D. Schwieters, Concordance of residual dipolar couplings, backbone order parameters and crystallographic B-factors for a small α/β protein: a unified picture of hight-probability, fast atomic motions in proteins, J. Mol. Biol. 355 (2006) 879–886.
[39] B. Vögeli, J. Orts, D. Strotz, P. Güntert, R. Riek, Discrete three-dimensional representation of macromolecular motion from eNOE-based ensemble calculation, Chimia 66 (2012) 787–790.
[40] B. Vögeli, The nuclear Overhauser effect from a quantitative perspective, Prog. Nucl. Magn. Reson. Spectrosc. 78 (2014) 1–46.
[41] C.B. Post, Internal motional averaging and three-dimensional structure determination by nuclear magnetic resonance, J. Mol. Biol. 224 (1992) 1087–1101.
[42] K. Houben, R. Boelens, Side chain dynamics monitored by 13C-13C cross-relaxation, J. Biomol. NMR 29 (2004) 151–166.
[43] L.E. Kay, G.M. Clore, A. Bax, A.M. Gronenborn, Four-dimensional heteronuclear triple-resonance NMR spectroscopy of Interleukin-1β in solution, Science 249 (1990) 411–414.
[44] M.J. Bostock, D.J. Holland, D. Nietlispach, Compressed sensing reconstruction of undersampled 3D NOESY spectra: application to large membrane proteins, J. Biomol. NMR 54 (2012) 15–32.
[45] V. Tugarinov, L.E. Kay, I. Ibraghimov, V.Y. Orekhov, High-resolution four-dimensional 1H-13C NOE spectroscopy using methyl-TROSY, sparse data acquisition, and multidimensional decomposition, J. Am. Chem. Soc. 127 (2005) 2767–2775.
[46] B.E. Coggins, J.W. Werner-Allen, A. Yan, P. Zhou, Rapid protein global fold determination using ultrasparse sampling, high-dynamic range artifact suppression, and time-shared NOESY, J. Am. Chem. Soc. 134 (2012) 18619–18630.
[47] A.T. Brünger, G.M. Clore, A.M. Gronenborn, R. Saffrich, M. Nilgens, Assessing the quality of solution nuclear magnetic resonance structures by complete cross-validation, Science 261 (1993) 328–331.
[48] W. Rieping, M. Habeck, M. Nilgens, Inferential structure determination, Science 309 (2005) 303–306.
[49] S. Olsson, J. Frellsen, W. Boomsma, K.V. Mardia, T. Hamelryck, Inference of structure ensembles from sparse, averaged data, PLoS ONE 8 (2013) e79439.
[50] H.J. Dyson, P.E. Wright, Unfolded proteins and protein folding studied by NMR, Chem. Rev. 104 (2004) 3607–3622.
[51] H. Nguyen, M. Jäger, A. Moretti, M. Gruebele, J.W. Kelly, Tuning the free-energy landscape of a WW domain by temperature, mutation, and truncation, Proc. Natl. Acad. Sci. USA 100 (2003) 3948–3953.
[52] F. Liu, D. Du, A.A. Fuller, J.E. Davoren, P. Wipf, J.W. Kelly, M. Gruebele, An experimental survey of the transition between two-state and downhill protein folding scenarios, Proc. Natl. Acad. Sci. USA 105 (2008) 2369–2374.
[53] D. Klimov, D. Thirumalai, Mechanisms and kinecitcs of beta-hairpin formation, Proc. Natl. Acad. Sci. USA 97 (2000) 2544–2549.
[54] D.E. Shaw, P. Maragakis, K. Lindorff-Larsen, S. Piana, R.O. Dror, M.P. Eastwood, J.A. Bank, J.M. Jumper, J.K. Salmon, Y. Shan, W. Wriggers, Atomic-level characterization of the structural dynamics of proteins, Science 330 (2010) 341–346.
[55] M. Jäger, H. Nguyen, J.C. Crane, J.W. Kelly, M. Gruebele, The folding mechanism of a β-sheet: the WW domain, J. Mol. Biol. 311 (2001) 373–393.
[56] S.A. Beccara, T. Škrbić, R. Covino, P. Faccioli, Dominant folding pathways of a WW domain, Proc. Natl. Acad. Sci. USA 190 (2012) 2330–2335.
[57] G. Ibragimova, R. Wade, Stability of the beta-sheet of the WW domain: a molecular dynamics simulation study, Biophys. J. 77 (1999) 2191–2198.
[58] H. Wang, S.-S. Sung, Molecular dynamics simulations of three-stranded β-sheet folding, J. Am. Chem. Soc. 122 (2000) 1999–2009.
[59] K. Lindorff-Larsen, S. Piana, R.O. Dror, D.E. Shaw, How fast-folding proteins fold, Science 334 (2011) 517–520.
[60] D.M. Korzhnev, T.L. Religa, L.E. Kay, Transiently populated intermediate functions as a branching point of the FF domain folding pathway, Proc. Natl. Acad. Sci. USA 109 (2012) 17777–17782.
[61] I. Bezsonova, A. Singer, W.-Y. Choy, M. Tollinger, J.D. Forman-Kay, Structural comparison of the unstable drkN SH3 domain and a stable mutant, Biochemistry 44 (2005) 15550–15560.
[62] H.J. Dyson, P.E. Wright, Intrinsically unstructured proteins and their functions, Nat. Rev. Mol. Cell Biol. 6 (2005) 197–208.
[63] M. Vendruscolo, Enzyme activity in disordered states of proteins, Curr. Opin. Chem. Biol. 14 (2010) 671–675.
[64] O. Zhang, L.E. Kay, D. Shortle, J.D. Forman-Kay, Comprehensive NOE characterization of a partially folded large fragment of staphylococcal nuclease Δ131Δ, using NMR methods with improved resolution, J. Mol. Biol. 272 (1997) 9–20.
[65] Y.K. Mok, C.M. Kay, L.E. Kay, J. Forman-Kay, NOE data demonstrating a compact unfolded state for an SH3 domain under non-denaturing conditions, Journal of Molecular Biology 289 (1999) 619–638.
[66] E. Barbar, NMR characterization of partially folded and unfolded conformational ensembles of proteins, Biopolymers 51 (1999) 191–207.
[67] H. Sticht, P. Bayer, D. Willbold, S. Dames, C. Hilbich, K. Beyreuther, R.W. Frank, P. Rösch, Structure of amyloid A4-(1-40)-peptide of Alzheimer's disease, Eur. J. Biochem. 233 (1995) 293–298.
[68] R. Riek, P. Güntert, H. Döbeli, B. Wipf, K. Wüthrich, NMR studies in aqueous solution fail to identify significant conformational differences between the monomeric forms of two Alzheimer peptides with widely different plaque-competence, Aβ(1-40)ox and Aβ (1-42)ox, Eur. J. Biochem. 268 (2001) 5930–5936.
[69] O. Crescenzi, S. Tomaselli, R. Guerrini, S. Salvadori, A.M. D'Ursi, P.A. Temussi, D. Picone, Solution structure of the Alzheimer amyloid β-peptide (1-42) in an apolar microenvironment, Eur. J. Biochem. 269 (2002) 5642–5648.
[70] J. Danielsson, A. Andersson, J. Jarvet, A. Gräslund, 15N relaxation study of the amyloid β-peptide: structural propensities and peristence length, Magn. Reson. Chem. (2006) S114–S121.
[71] J.L. Kofron, P. Kuzmic, V. Kishore, E. Colón-Bonilla, D.H. Rich, Determination of kinetic constants for peptidyl prolyl cis-trans isomerases by an improved spectrophotometric assay, Biochemistry 30 (1991) 6127–6134.
[72] D. Kern, G. Kern, G. Scherer, G. Fischer, T. Drakenberg, Kinetic analysis of cyclophilin-catalyzed prolyl cis/trans isomerization by dynamic NMR spectroscopy, Biochemistry 34 (1995) 13594–13602.
[73] E.Z. Eisenmesser, O. Millet, W. Labeikovsky, D.M. Korzhnev, M. Wolf-Watz, D.A. Bosco, J.J. Skalicky, L.E. Kay, D. Kern, Intrinsic dynamics of an enzyme underlies catalysis, Nature 438 (2005) 117–121.
[74] M.A. Wear, M.D. Walkinshaw, Thermodynamics of the cyclophilin-A/cyclosporine-A interaction: a direct comparison of parameters determined by surface plasmon resonance using Biacore T100 and isothermal titration calorimetry, Anal. Biochem. 359 (2006) 285–287.
[75] E.Z. Eisenmesser, D.A. Bosco, M. Akke, D. Kern, Enzyme dynamics during catalysis, Science 295 (2002) 1520–1523.
[76] D. Kern, E.Z. Eisenmesser, M. Wolf-Watz, Enzyme dynamics during catalysis measured by NMR spectroscopy, Methods Enzymol. 394 (2005) 507–524.
[77] J.S. Fraser, M.W. Clarkson, S.C. Degnan, R. Erion, D. Kern, T. Alber, Hidden alternative structures of proline isomerase essential for catalysis, Nature 462 (2009) 669–673.
[78] P. Jemth, S. Gianni, PDZ domains: folding and binding, Biochemistry 46 (2007) 8701–8708.
[79] H.J. Lee, J.J. Zheng, PDZ domains and their binding partners: structure, specify, and modification, Cell Commun. Signal 8 (2010) 1–18.
[80] S.W. Lockless, R. Ranganathan, Evolutionary conserved networks of energetic connectivity in protein families, Sciences 286 (1996) 295–299.
[81] R.I. Dima, D. Thirumalai, Determination of network of residues that regulate allostery in protein families using sequence analysis, Protein Sci. 15 (2006) 258–268.
[82] G. Gianni, T. Walma, A. Arcovito, N. Calcosci, A. Bellelli, A. Engstrom, C. Travaglinilocatelli, M. Brunori, P. Jemth, G.W. Vuister, Demonstration of long-range interactions in a PDZ domain by NMR, Kinet.Protein Eng. Struct. 14 (2006) 1801–1809.
[83] E.J. Fuentes, S.A. Gilmore, R.V. Mauldin, A.L. Lee, Evaluation of energetic and dynamic coupling networks in a PDZ domain protein, J. Mol. Biol. 364 (2006) 337–351.
[84] C.N. Chi, L. Elfström, Y. Shi, T. Snäll, A. Engström, P. Jemth, Reassessing a sparse energetic network within a single protein domain, Proc. Natl. Acad. Sci. USA 105 (2008) 4679–4684.
[85] G. Hultqvist, S.R. Haq, A.S. Punekar, C.N. Chi, Å. Engström, A. Bach, K. Strømgaard, M. Selmer, S. Gianni, P. Jemth, Energetic pathway sampling in a protein interaction domain, Structure 21 (2013) 1193–1202.
[86] E.J. Fuentes, C.J. Der, A.L. Lee, Ligand-dependent dynamics and intramolecular signaling in a PDF domain, J. Mol. Biol. 335 (2005) 1105–1115.
[87] X. Niu, Q. Chen, J. Zhang, W. Shen, Y. Shi, J. Wu, Interesting structural and dynamical behaviors exhibited by the AF-6 PDZ domain upon Bcr peptide binding, Biochemistry 46 (2007) 15042–15053.
[88] A.B. Law, E.J. Fuentes, A.L. Lee, Conservation of side-chain dynamics within a protein family, J. Am. Chem. Soc. 131 (2009) 6322–6323.
[89] A. Dhulesia, J. Gsponer, M. Vendruscolo, Mapping of two networks of residues that exhibit structural and dynamical changes upon binding in a PDZ domain protein, J. Am. Chem. Soc. 130 (2008) 8931–8939.
[90] C. Eichmann, J. Orts, C. Tzitzilonis, B. Vögeli, J.L. Lorieau, R. Riek, Intermolecular detergent – membrane protein NOEs for the characterization of dynamics for membrane protein–detergent complexes, submitted for publication.
[91] J.L. Lorieau, J.M. Louis, C.D. Schwieters, A. Bax, PH-triggered, activated-state conformations of the influenza hemagglutinin fusion peptide revealed by NMR, Proc. Natl. Acad. Sci. USA 109 (2012) 19994–19999.